Estimating day of the estrous cycle

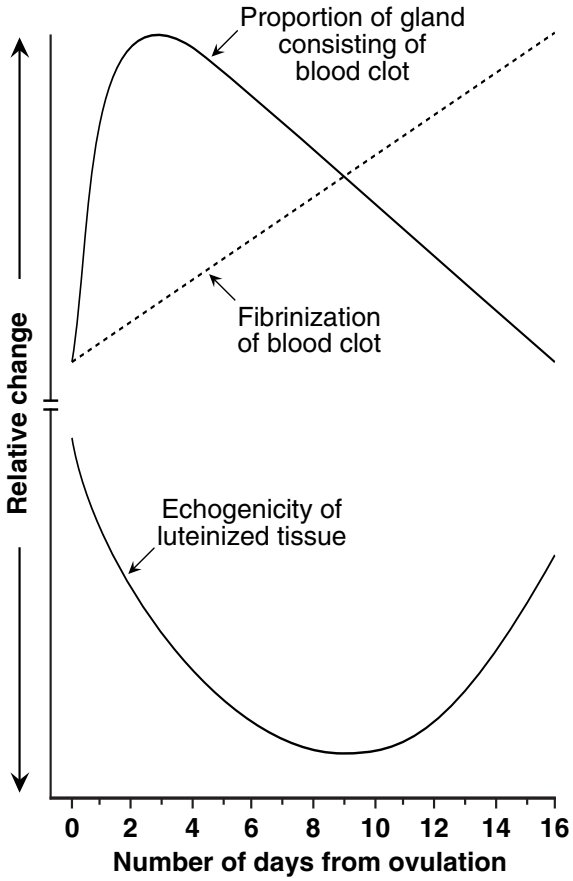

Summary of changes in luteal ultrasonic morphology during the estrous cycle. The luteal and follicular phases of the estrous cycle can be readily identified on the basis of the presence of a corpus luteum (luteal phase) or a large follicle in the absence of a corpus luteum (follicular phase). During the luteal phase, echogenicity of the luteal tissue can be used to help estimate the age of either a solid or a centrally hemorrhagic corpus luteum (pg 80). Often echogenicity is high (hyperechogenic) during luteal development (first few days after ovulation) and again during regression (last few days). The first few days usually can be distinguished from the last few days on the basis of gland size; the echogenicity on the last few days is associated with increased density of the gland due to luteal regression. The echogenicity criterion does not always apply, however. In a series of daily examinations of 55 luteal glands in Quarter Horses, 12% were not hyperechogenic during development and 64% were not hyperechogenic during regression *(176)*. About 50% of luteal glands develop a blood-filled central cavity that is more than 10% of the cross-sectional area of the corpus luteum. The ratio of luteal tissue to blood clot and the degree of organization of the clot (network of echogenic bands) can be used to help estimate the age of such glands, as shown. The blood clots develop during the first few days and then progressively become more organized and proportionally smaller (pg 81). Follicular diameters (pg 47) and ultrasonically detectable edema of the endometrial folds (pg 94) provide further information for estimating day of the estrous cycle. During estrous behavior, follicles ≥30 mm are highly correlated with high circulating estradiol and low progesterone *(128)*.

Origin of Specular Echoes

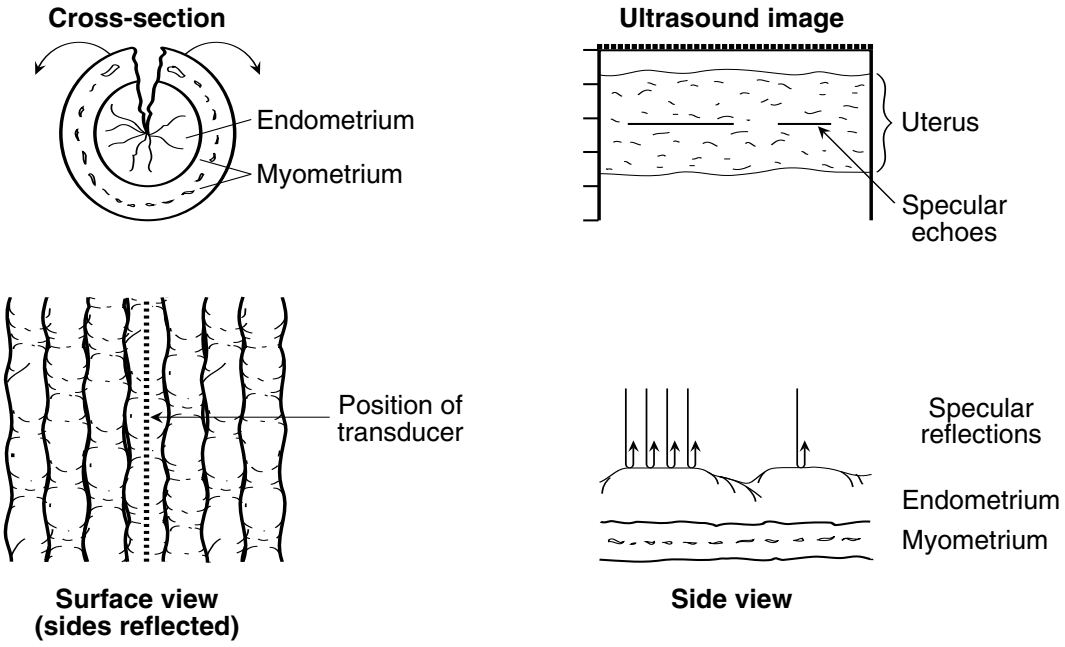

Drawings of various views of uterine folds. Note the longitudinal arrangement of the uterine folds in the view of the internal surface. The surface of the folds is shown photographically (pg 18). There are seven major folds *(140)*. During the estrous cycle and early pregnancy, the folds are relatively prominent, whereas during the anovulatory season, the folds are not. Specular echoes are caused by the reflection of ultrasound pulses from a smooth surface that is wider than the pulse and is parallel to the face of the transducer (Bk1-66). Because these conditions can be met by a portion of the surfaces of endometrial folds, the bright white lines seen in images of longitudinal views of the uterus are attributable to specular echoes. As shown in the diagram, specular echoes appear on the image for those portions of the folds that are parallel to the transducer face. Sometimes long continuous lines may be seen; at other times there may be short, interrupted segments or no lines. During deep anestrus, the folds may not be prominent enough to act as specular reflectors. The reason for the decrease in specular echoes during estrus is not known. Perhaps the engorged folds are less likely to present a long, smooth, uninterrupted surface parallel to the transducer.

Ultrasonic Anatomy of Placental Sacs over Days 16 to 50

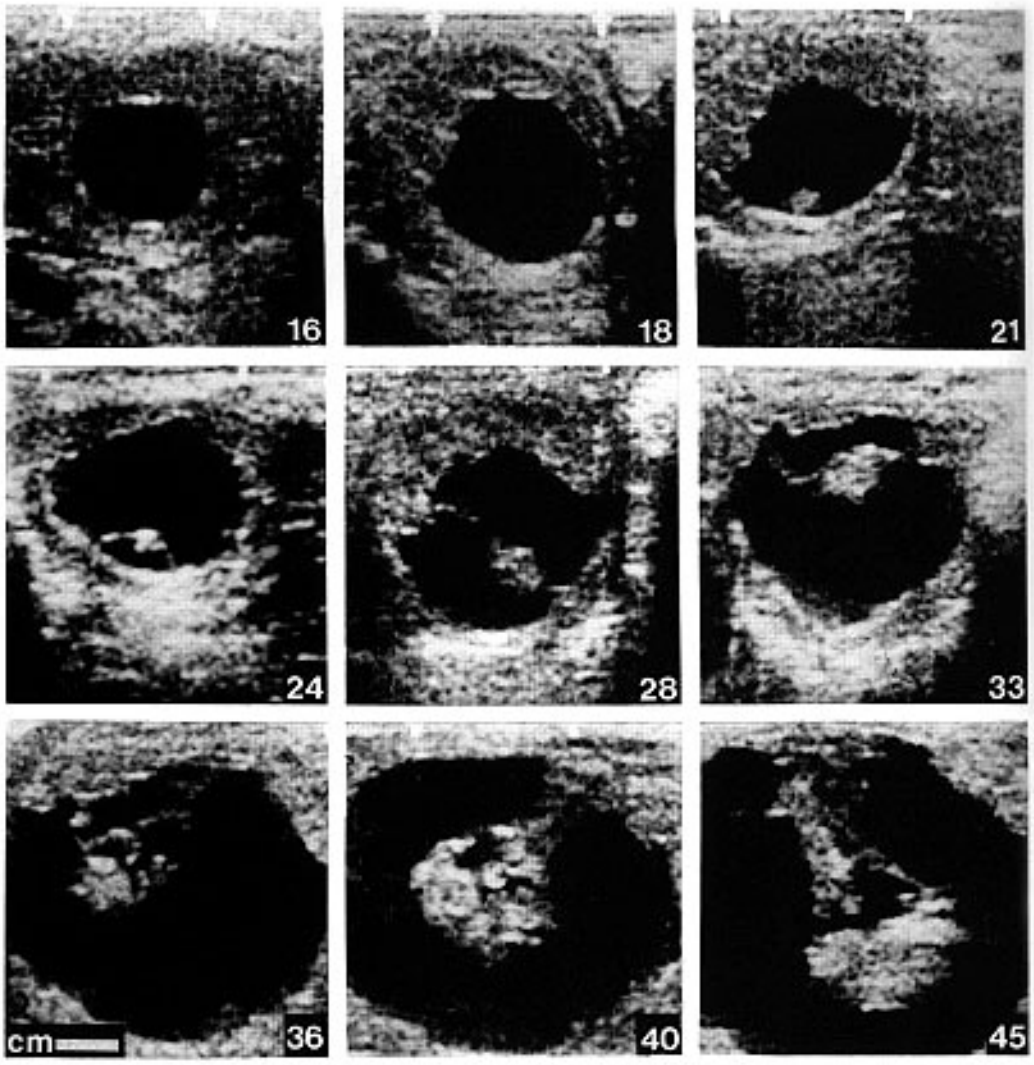

Ultrasound images and diagrammatic review (facing page) showing ascent of embryo and descent of fetus. After fixation on Day 15 or 16, the vesicle begins to lose its spherical shape. The dorsal endometrial folds hypertrophy, so that the image of the vesicle is sometimes guitar-pick-shaped with the apex oriented dorsally. The embryo proper usually becomes ultrasonically visible by Day 20 as a small (4 mm) echogenic spot on the curved ventral aspect of the vesicle. The allantoic sac usually is well-defined ventral to the embryo by Day 24. As shown for Days 24 to 33, the allantoic sac (ventral) and yolk sac (dorsal) are separated by an echogenic line (apposed walls of the two placental sacs). The embryo is the enlarged hyperechogenic nodule on the separating line.

expansion curve. The confidence intervals were 3 days for 6 to 23 mm vesicles and 8 days for 27 to 56 mm vesicles. By following the dotted line from an observed height across to the linear regression line and then down to the day scale, age can be estimated (95% accuracy) within ±1.5 days for 6 to 23 mm vesicles and ±4 days for 27 to 56 mm vesicles. During the S-shaped portion of the curve (Days 16 to 28), the cross-sectional height did not change enough to be an adequate indicator of age. However, profound morphologic changes occurred during this time.

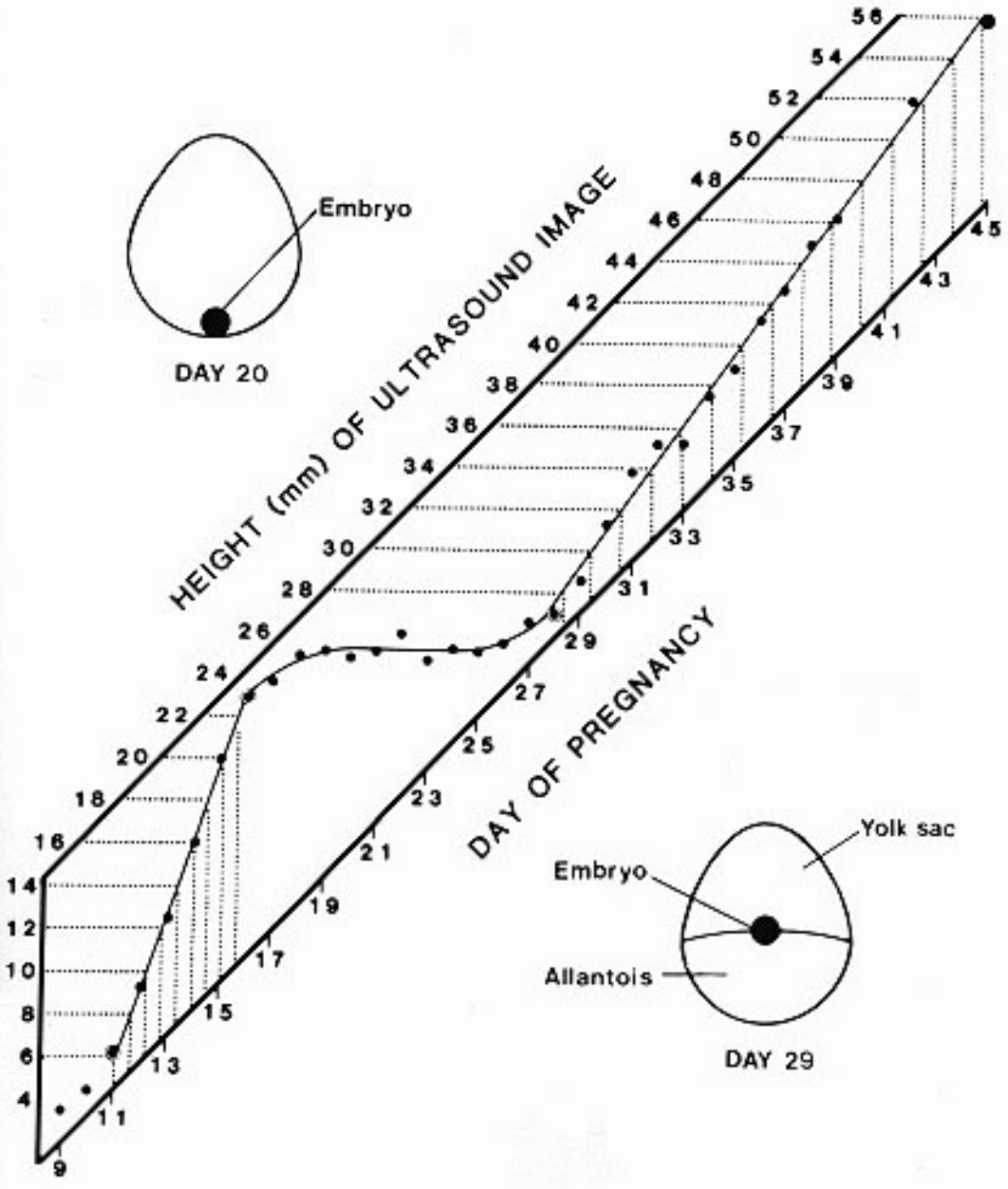

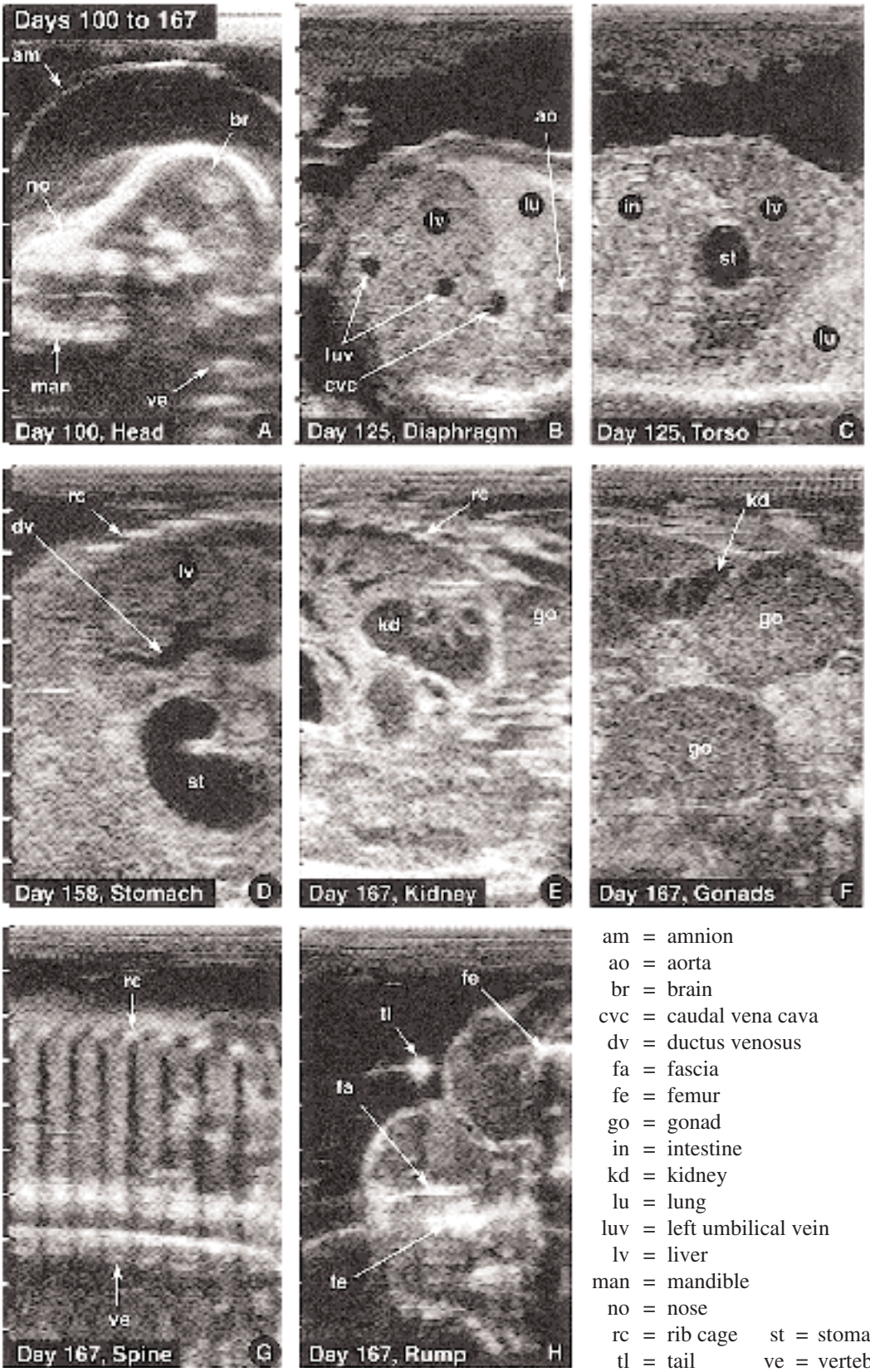

am = amnion
ao = aorta
br = brain
cvc = caudal vena cava
dv = ductus venosus
fa = fascia
fe = femur
go = gonad
in = intestine
kd = kidney
lu = lung
luv = left umbilical vein
lv = liver
man = mandible
no = nose
rc = rib cage
st = stomach
tl = tail
ve = vertebra

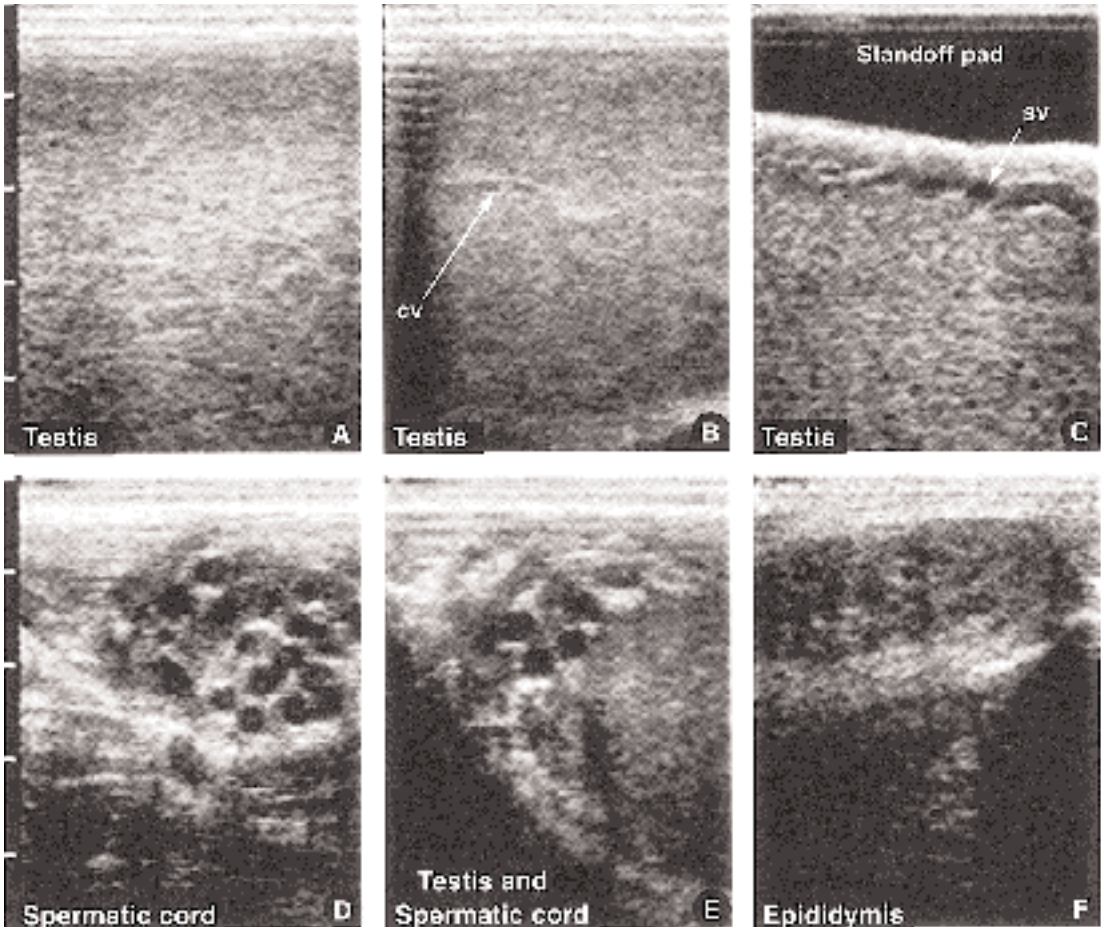

Testis and associated structures.

(A) Cross section of a testis taken with the probe vertical on the lateral testicular surface and pointing upward; the echotexture of the parenchyma is uniform.

(B) The central vein (cv) is detectable, especially in the cranial portion of the testis.

(C) A standoff pad (anechoic area) was used between the transducer and ventral scrotum to highlight the superficial vessels (sv) of the testicular artery. These vessels are most prominent at the caudal portion of the testis.

(D) The many blood vessels (pampiniform plexus) of the spermatic cord are shown in cross section.

(E) Area of attachment of the spermatic cord to the testis.

(F) Epididymis near the tail imaged with the transducer placed longitudinally on the organ; the anechoic areas represent sections of the convoluted epididymal duct. The epididymis has larger hypoechoic areas than does the testis.